



OPEN ACCESS

EDITED BY
Dan Lu,
Alfred University, United States

REVIEWED BY
Jiaming Luo,
Southwest Jiaotong University, China
Yue Wang,
Northeast Electric Power University,
China
Shuai Chu,
Shenyang University of Technology,
China

*CORRESPONDENCE
Bo Ye,
bby90031@163.com

SPECIALTY SECTION
This article was submitted to Smart
Grids,
a section of the journal
Frontiers in Energy Research

RECEIVED 04 July 2022
ACCEPTED 19 July 2022
PUBLISHED 16 August 2022

CITATION
Ye B, Li F, Li M, Yan P, Yang H and Wang L
(2022), Intelligent detection method for
substation insulator defects based
on CenterMask.
Front. Energy Res. 10:985600.
doi: 10.3389/fenrg.2022.985600

COPYRIGHT
© 2022 Ye, Li, Li, Yan, Yang and Wang.
This is an open-access article
distributed under the terms of the
[Creative Commons Attribution License
\(CC BY\)](https://creativecommons.org/licenses/by/4.0/). The use, distribution or
reproduction in other forums is
permitted, provided the original
author(s) and the copyright owner(s) are
credited and that the original
publication in this journal is cited, in
accordance with accepted academic
practice. No use, distribution or
reproduction is permitted which does
not comply with these terms.

Intelligent detection method for substation insulator defects based on CenterMask

Bo Ye*, Feng Li, Mingxuan Li, Peipei Yan, Huiting Yang and Lihua Wang

State Grid Xinjiang Electric Power Research Institute, Urumqi, China

With the development of intelligent operation and maintenance of substations, the daily inspection of substations needs to process massive video and image data. This puts forward higher requirements on the processing speed and accuracy of defect detection. Based on the end-to-end learning paradigm, this article proposes an intelligent detection method for substation insulator defects based on CenterMask. First, the backbone network VoVNet is improved according to the residual connection and eSE module, which effectively solves the problems of deep network saturation and gradient information loss. On this basis, an insulator mask generation method based on a spatial attention-directed mechanism is proposed. Insulators with complex image backgrounds are accurately segmented. Then, three strategies of pixel-wise regression prediction, multi-scale features, and centerness are introduced. The anchor-free single-stage target detector accurately locates the defect points of insulators. Finally, an example analysis is carried out with the substation inspection image of a power supply company in a certain area to verify the effectiveness and robustness of the proposed method.

KEYWORDS

smart substation, CenterMask, insulator defect detection, instance segmentation, image processing

1 Introduction

In China, the “State Grid Corporation Artificial Intelligence Technology Application 2021 Work Plan” has made clear instructions to build and operate two levels of AI “two libraries and one platform” and form a number of high-precision and high-value power-specific models. As an important and indispensable part of the power system, the safe and stable operation of substations is the basis for building a strong smart grid (Han et al., 2021; Li et al., 2022a). Today, rising renewable energy uncertainty (Li et al., 2022b; Li et al., 2022c) and concerns about cyber security and privacy issues (Li et al., 2019; Li et al., 2022d) pose new challenges for substation operations. Therefore, there are strict standards for operation and maintenance (Q&M) of substation equipment (Huang et al., 2016).

Insulators are key equipment in substations. Common types include pillar insulators, bushing insulators, and suspension insulators. Its operational performance is directly related to the stable and continuous operation of the regional power grid. However,

insulator fouling and breakage are the main factors affecting its operational performance (He and Gorur, 2017). In order to meet the needs of Q&M, the substation is equipped with inspection robots and deployed a large number of high-definition cameras (Guan et al., 2021). The daily Q&M of insulators in the station needs to process massive amounts of video and image data. How to use data to efficiently analyze insulator defects is not only the focus of Q&M work but also the difficulty in defect detection (Wang et al., 2017).

Currently, scholars around the world have extensively investigated on the defect detection of substation insulators as artificial intelligence has been successfully applied to classification problems in engineering (Shi et al., 2008; Shi et al., 2009). In Zhai et al. (2018), based on machine vision, the feature extraction of the insulator image is completed through the Vision module of LabVIEW, and the preliminary identification and positioning of the insulator are realized. The surface of substation insulators is very susceptible to the influence of wet weather, resulting in contamination and flashover accidents in substation facilities. Tang et al. (2020) designed an insulator cleaning robot based on binocular vision, using the YOLOv4-tiny deep learning network algorithm to identify and detect pillar insulators and flange targets. By establishing an electrothermal conversion model for insulator strings, a method for identifying deteriorating porcelain insulators in substations based on infrared thermal imaging technology is proposed. The method in Zhang and Chen (2020) obtains a degree of practicality. In addition, the method in Gao et al. (2021) was used in order to improve the fault diagnosis capability of substation equipment insulators. A method for identifying breakage of substation equipment insulators based on intelligent image information fusion and edge contour segmentation detection is proposed. Usamentiaga et al. (2018) studied multi-source image information fusion detection and the multi-source image fusion reconstruction method of the insulator contamination state. However, this work extracts the surface color features, temperature rise features, and discharge intensity features of insulators from visible light images, infrared images, and ultraviolet images, respectively, which makes the detection method difficult to apply online (Jin et al., 2018).

In summary, the application of computer vision and deep learning methods to realize defect detection of substation insulators has become a research hotspot. However, the existing methods are not ideal for the detection of massive high-definition image data in substations, and there is a common problem of low real-time detection of insulator defects. Therefore, an end-to-end agile detection method for substation insulator defects is proposed. The method is based on a single-stage instance segmentation algorithm and adopts an end-to-end learning paradigm.

The main novelties of this work are as follows:

- (i) The end-to-end design idea revolutionizes the staged and step-by-step segmentation and detection methods in traditional insulator detection research. This strategy effectively reduces the impact of step-by-step error iteration on model performance.
- (ii) Insulator mask generation and defect detection can be performed in parallel. This method greatly improves the fault identification efficiency of the piece of equipment Q&M in the substation.
- (iii) The one-stage instance segmentation algorithm has been successfully applied in the detection of insulator defect points by introducing pixel-by-pixel regression prediction, multi-scale features, and centerness, the three strategies to accurately output the bounding box label of the defect point location.

This article is organized as follows: Section 2 briefly describes the architecture for agile detection of insulator defect points in substations. The method of insulator mask generation and defect point detection is described in detail in Section 3. Section 4 verifies the effectiveness of the proposed method based on the built experimental environment. Finally, conclusions and outlook are presented in Section 5.

2 Architecture of the insulator defect intelligent detection method

Due to the close connection between the equipment in the substation, the insulator image taken by the inspection robot is mixed with more other pieces of transformer equipment (Wang and Meng, 2019; Kou et al., 2022). This makes it necessary to step through the images during insulator defect detection. However, the result of step-by-step processing will certainly increase the detection time and reduce the accuracy of detection (Chen et al., 2019; Zhao et al., 2019). At the same time, the characteristics of the massive amount of inspection images are different to ignore. Therefore, this study comprehensively measures the Q&M requirements of substation insulators and the training complexity of massive inspection images. A defect detection method based on CenterMask is designed. The overall implementation plan of this work is shown in Figure 1. Based on the one-stage target detection algorithm, a parallelized image segmentation technique is incorporated to obtain the insulator mask (Yuan et al., 2021). The masks for insulator defect points are also extracted separately. By counting the insulator defect detection task points, the main tasks are insulator detection, insulator mask segmentation, insulator defect point detection, and insulator defect point location.

As shown in Figure 1, this end-to-end work can be decomposed into three parts. First, based on the accumulated original inspection images, the initial image database is constructed. Then, the defect detection model structure is designed. This part is also the core of the whole method. 1) The backbone network adopts improved VoVNet to achieve

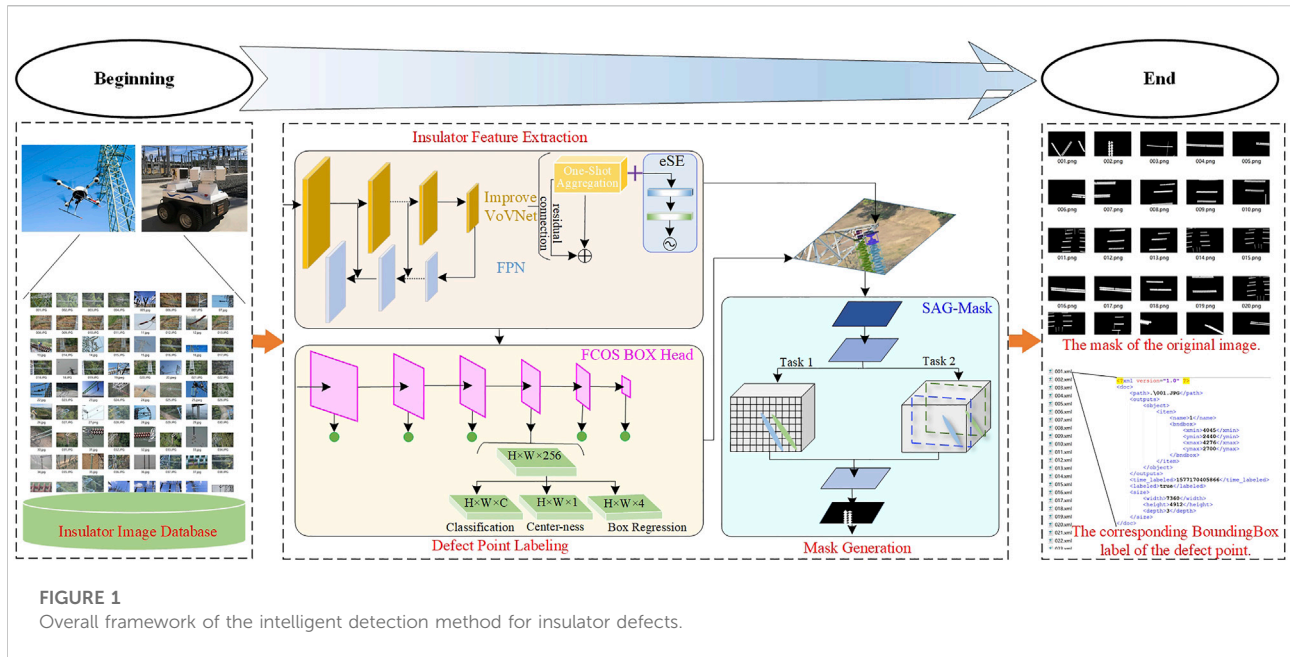


FIGURE 1 Overall framework of the intelligent detection method for insulator defects.

efficient extraction of target features. 2) The spatial attention-guided mask (SAG-mask) branch generates target masks. 3) Using fully convolutional one-stage (FCOS) to detect defect points of insulators. Finally, the end realizes the output of the insulator mask and the bounding box label of the defect point.

3 Agile detection method for substation insulator defects

CenterMask is a newer instance segmentation algorithm proposed by Youngwan Lee and Jongyoul Park of the Korea Institute of Electronics and Communications in 2019 (Lee and Park, 2020). This algorithm adds the SAG-mask module invented by scholars to the famous one-stage anchor-free target detection algorithm FCOS, which makes its target segmentation accuracy and speed superior to traditional algorithms. The two scholars made the algorithm open source for scholars in the field of image and vision to jointly explore the application research of the algorithm. The application of this algorithm in substation insulator defect detection further improves the intelligence and accuracy of insulator defect detection.

3.1 Insulator feature extraction based on improved VoVNet

The inspection robot in the smart substation will collect images of insulators from different angles during the operation. The background of the insulator in the image is complex and diverse, which has serious noise interference to the accurate

detection of insulator defect points (Tao et al., 2018; Kou et al., 2020a). Therefore, our first task is to achieve accurate extraction of insulator target features. It is the backbone network of the model that accomplishes this task in the study.

At present, various target detection models rely on different backbone networks (Du et al., 2021). The core module used by the mainstream target detection model DenseNet is the dense block. All previous layers are aggregated through dense connections, resulting in a linear increase in the number of input pipelines for each subsequent layer. This strategy makes the memory access cost and energy consumption extremely high, and the computing speed is seriously hindered (Xu and Wu, 2020). When the input is a higher-quality insulator image, object extraction tends to consume more memory and inference time. This problem makes the detection effect of insulator defects far from meeting the standard of massive high-definition insulator images in substations. The CenterMask backbone network proposed by the research utilizes an improved VoVNet. The short board of feature redundancy caused by dense connections in DenseNet is effectively solved, and the core module of one-shot aggregation (OSA) is adopted. In the strategy, all the previous layers are unified and aggregated at the end.

The improved VoVNet addresses the performance saturation problem and the information loss problem in standard VoVNet, respectively. 1) By adjusting the input of the OSA module and adding it to the output, the residual link of ResNet is introduced to ensure that VoVNet can train a deeper network. It can effectively process insulator images with high pixel ratios. 2) The eSE module of ResNet is added to the last feature layer of VoVNet, and the two fully connected layers used in the original SE module are directly replaced by one, which effectively reduces

the loss of channel information. This method further enhances the feature extraction capability of the insulator target. The improved connection structure of OSA modules in VoVNet according to the idea is shown in the insulator feature extraction area in Figure 1. The performance of the target detection models based on the improved VoVNet surpasses the models based on other target detection algorithms. The algorithm greatly improves the GPU computing efficiency and meets the needs of high-speed processing for intelligent identification of hidden dangers of insulators.

3.2 Insulator mask extraction based on the spatial attention-guided mask

Insulator image datasets mostly suffer from the problems of complex backgrounds, multiple strings in a single image, and insulator overlap (Kou et al., 2020b). Section 3.1 shows how insulator feature extraction realizes insulator target detection. The position of the insulator in the image is accurately framed, and only completing this link cannot quickly detect the defect points of the insulator. Therefore, it is necessary to further realize the precise segmentation of insulator beads on this basis. Adding the SAG-mask branch to the target result of FCOS detection in the CenterMask algorithm satisfactorily completes this task.

The most famous ones in instance segmentation are Mask RCNN and its related improved algorithms, as well as the YOLACT algorithm which focuses on speed (Wang et al., 2020b). However, a spatial attention-oriented mechanism is proposed in CenterMask. The mechanism is able to utilize the spatial attention map of the input image to predict segmentation masks for each boxed instance. The added SAG-mask branch can be performed in parallel with the insulator fault point identification of the target detector, which greatly improves the identification efficiency of intelligent hidden dangers of insulators.

In this article, the instance segmentation of insulators is decomposed into two simple and parallel subtasks, as shown in the mask generation area in Figure 1. Task 1 achieves the goal of constraining the local area of each insulator and naturally distinguishing the instance. A rough shape prediction is made around the center point of each insulator. Task 2 achieves precise segmentation of insulators while retaining the spatial position of precise segmentation. The branch is predicted using the insulator saliency pixels in the entire inspection image. The core idea is to focus on specific block features in the feature map by using an attention mechanism. Finally, a mask for each insulator's corresponding image position is constructed by multiplying the outputs of the two parallel branches.

The mathematical process of the instance segmentation process can be described as follows: the input insulator feature map is marked as $X_i \in R^{C \times H \times W}$. It is pooled using max pooling and average pooling. The pooled features are, respectively,

$F_{\max_pooling}, F_{\text{average_pooling}} \in R^{1 \times H \times W}$ and subsequently passed through a 3×3 convolutional neural network. The specific mathematical functions are as follows:

$$A(\text{sag}(X_i) = \sigma F_{3 \times 3}(P_{\max_pooling} \cdot P_{\text{average_pooling}})). \quad (1)$$

Then, saliency pixels are used in task 2 to enhance the input features of the original insulator image, as shown in Eq. 2.

$$X_{\text{sag}} = A_{\text{sag}}(X_i) \otimes X_i. \quad (2)$$

3.3 Identification and location of insulator defects based on fully convolutional one-stage algorithm

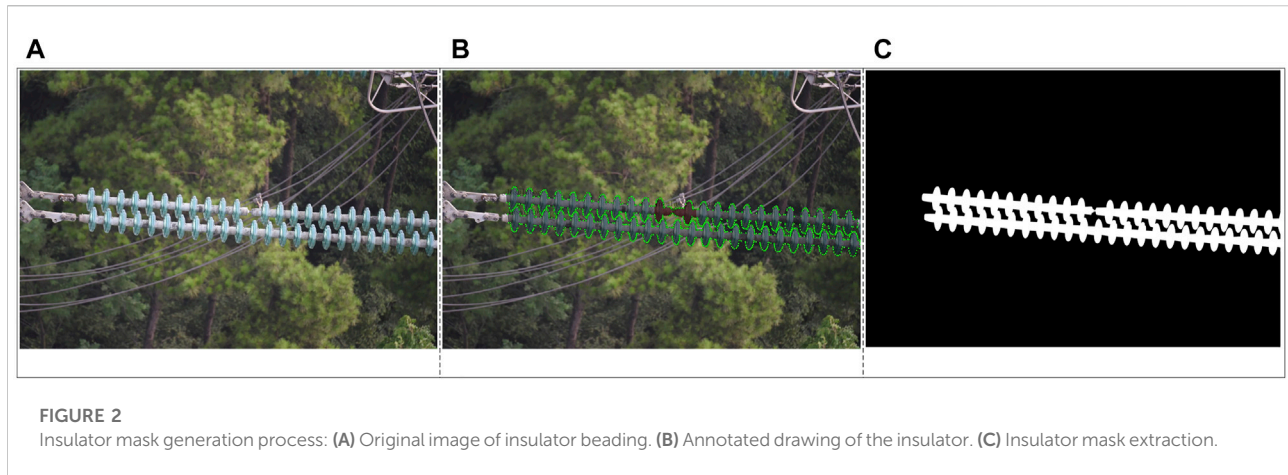
The goal of intelligent hidden danger identification of insulators is to quickly locate various common faults of insulators through intelligent algorithms, such as bead damage, excessive pollution, and aging cracks (Wang et al., 2020a). The accurate extraction of the insulator mask can only ensure that the location of the insulator is identified from the inspection image, and the insulator is accurately segmented. However, specific fault points require accurate location detection of the corresponding model. This work uses the anchor-free FCOS algorithm to complete the task in the target detection part of the overall CenterMask structure. FCOS is a fully convolutional one-stage object detection algorithm (Zhang et al., 2022). It solves the object detection problem in a pixel-by-pixel prediction manner. At the same time, in the detection process, the anchor-free box of FCOS is a huge advantage. The hyperparameters associated with anchor boxes and all the complex computations associated with anchor boxes are effectively avoided. The efficiency of insulator defect identification and location has been greatly improved. The output of the entire defect identification and localization results includes three aspects: pixel-by-pixel regression prediction, multi-scale features, and centerness.

The specific process framework is shown in the defect point labeling area in Figure 1. The first output of the 3 output layers is the classification branch. $H \times W$ represents the size of the feature. C represents the number of categories. A position in the input inspection image can be mapped to a position on the feature, and the mapping function is as follows:

$$\left(\left[\frac{r}{2} \right] + p\hat{r}, \left[\frac{r}{2} \right] + qr \right), \quad (3)$$

where the coordinates (p, q) denote a specific location in the inspection image. r denotes the scaling between the feature map and the original inspection image. This function can represent the relationship between the position of the point on the feature map and the position of the point on the output image. This lays the groundwork for computing the classification and regression objectives for each point on the feature map.

The second output is the centerness policy. The FCOS algorithm is applied to achieve the high efficiency of one-stage anchor-free box



calculation and high recall rate of the pixel-by-pixel regression strategy. It also brings many low-quality prediction bounding boxes with very large deviation from the center point. By introducing this strategy, the distance between each point and the target center can be calculated, thereby suppressing some predicted bounding boxes that are far away from the target center. But this strategy does not introduce any excessive hyperparameters.

The centerness strategy adds a branch to each prediction layer of the feature pyramid. Also, this branch is parallel to the classification branch, which is equivalent to adding a loss function to the network. During the training process of the image dataset, the loss function constrains the predicted bounding box to be as close to the center point as possible so that the auxiliary non-maximum suppression (NMS) can filter out the low-quality bounding box prediction. The loss function is as follows:

$$Loss^* = \sqrt{\frac{\min(d_{left}^*, d_{right}^*)}{\max(d_{left}^*, d_{right}^*)} \times \frac{\min(d_{top}^*, d_{bottom}^*)}{\max(d_{top}^*, d_{bottom}^*)}} \quad (4)$$

where the distances from the center point to the left, right, top, and bottom sides of the prediction bounding box are represented by d_{left} , d_{right} , d_{top} , and d_{bottom} , respectively. $Loss^*$ is the value of the loss function, and the more it tends to zero, the better the prediction can be constrained.

The third output is the return branch. When performing the target frame regression on all the points in the target frame of defect points in the inspection image, the distance to each edge is used as the measurement standard. This part is the main difference between the target detection algorithm without the anchor frame and the target detection algorithm based on the anchor frame, where 4 in $H \times W \times 4$ represents four values related to regression. This is calculated as follows:

$$\begin{aligned} d_{left}^* &= m - m_0^{(i)}, d_{top}^* = n - n_0^{(i)}, \\ d_{right}^* &= m_0^{(i)} - m, d_{bottom}^* = n_0^{(i)} - n. \end{aligned} \quad (5)$$

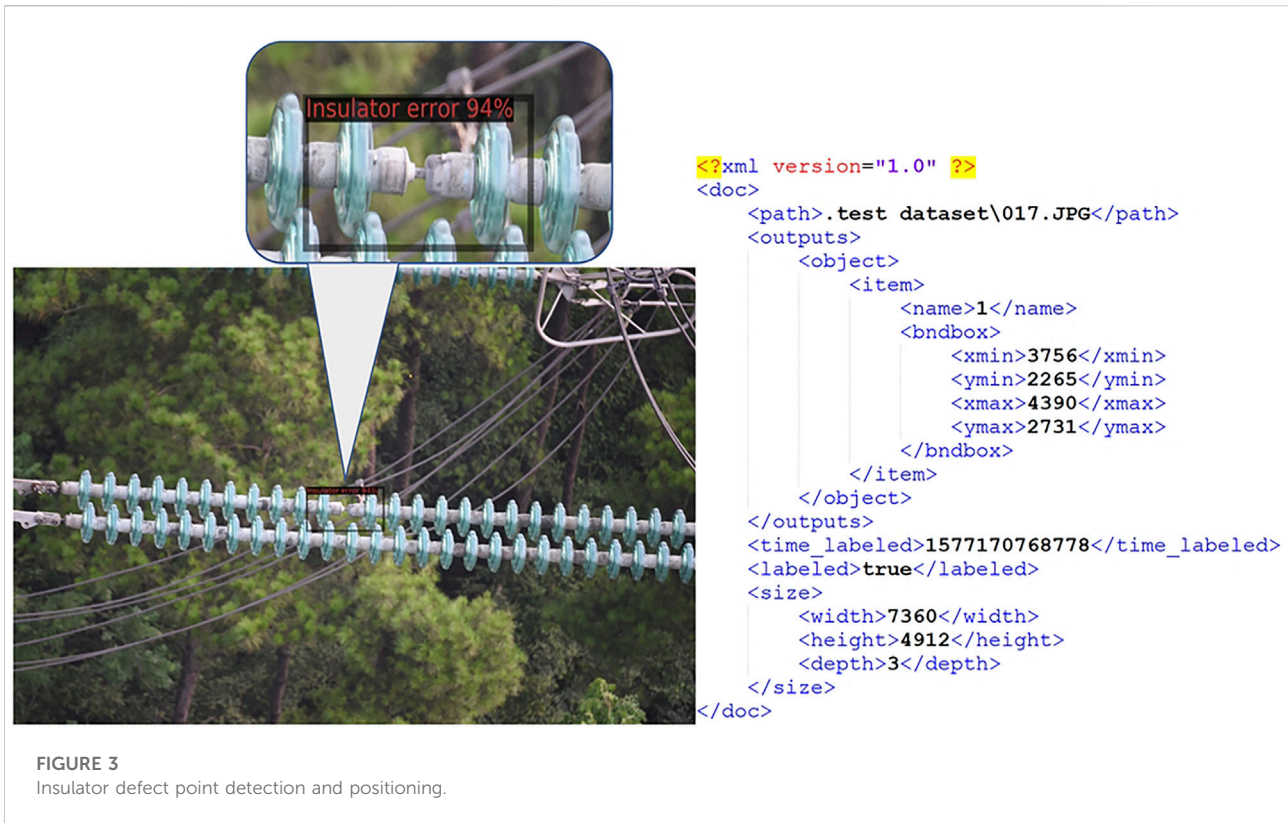
4 Case study

In order to verify the effectiveness and robustness of the insulator defect agile detection method proposed in this study, taking the substation inspection image of a power supply company in a certain area as an example, an example analysis is carried out. There are two main aspects to build the experimental environment in the DELL graphics workstation. Hardware: Intel(R) Xeon(R) Gold 5118 CPU @ 2.30 GHz, NVIDIA Quadro P5000, and 128 GB RAM; Software: Python 3.7.6, CUDA 10.1, PyTorch 1.4.0, Detectron2 0.1.1, and CV2 4.2.0. The model output results are evaluated by a number of index combinations to further realize the optimization of the defect point identification model.

4.1 Insulator mask generation and defect detection

The insulator images captured by the inspection are divided into the training set and test set. In the aforementioned experimental environment, the analysis of training set samples and the selection and optimization of the model backbone network are carried out. This model was trained over 200,000 iterations. During the training process, each part of the network loss is visualized to achieve accurate tuning of model parameters. The complete flow of insulator mask generation is shown in Figure 2.

First, the training set, as shown in Figure 2A, is manually annotated. It is used to assist the initial learning of the model. Figure 2B shows the manual annotation of the original inspection image using the labeling tool LabelMe. Insulators are marked with the “Insulator” label, and insulator defect points are marked with the “Insulator error” label. Then, the CenterMask network model is iteratively learned and adjusted using the effectively labeled training set. This process takes a long time. Finally, the trained insulator defect detection model is applied. The input test



set is used for model insulator mask extraction branch validity verification. The extracted rendering is shown in Figure 2C.

As mentioned in Section 2, defect point identification and mask extraction in the insulator defect detection model are two independent branches, and the two branches can be executed in parallel. The identification of defect points does not have to wait for mask generation or be disturbed by mask generation results. Therefore, the defect point identification and positioning is more flexible, and the effect is better. By adopting the same multi-scale training strategy as insulators, the model parameters are set for random scaling within the range of input scales. The insulator explosion point training dataset is enriched according to the maximum and minimum input size constraints. When outputting the defect point xml file, the visual output display of single-image insulator defect point identification and identification accuracy is realized. For the test set, the model insulator defect point detection visualization diagram and the corresponding positioning label stored in the xml file effect are shown in Figure 3.

4.2 Example index evaluation

For the model test results, the average precision (AP) and average recall (AR) evaluation metrics are set. Under the combination of different IOUs, areas under inspection (AREA), and number of objects under inspection (MaxDets), model

performance analysis is performed on all test results. The specific evaluation results are shown in Table 1. Here, IOU represents the degree of overlap between the generated candidate frame and the original marked frame. It is the ratio of intersection and union, and the calculation equation is as follows:

$$\text{IOU} = \frac{\text{Area of Overlap}}{\text{Area of Union}} \quad (6)$$

In Table 1, AP represents IOU ranging from 0.5 to 0.95. AP₅₀ represents the IOU range of 0.5–1.0. AP₇₅ represents the IOU range of 0.75–1.0. AP_s represents the AP measurement of the target box whose pixel area is smaller than 32². AP_m represents the AP measurement of the target box whose pixel area is between 32² ~ 96². AP_l represents the AP measurement of the target box whose pixel area is larger than 96². Value 1 represents the AP/AR generated by the insulator mask under different evaluation methods. Value 2 represents the index result value of defect point detection in different situations.

Analysis of Table 1 shows that when 0.5 is used as the IOU threshold for segmentation, the model mask generation effect is the best. The accuracy of the model is 93.4%, indicating that the model satisfies the extraction of insulators in most inspection image scenarios. However, the AP and AR of target boxes with a pixel area smaller than are significantly lower, indicating that the model still needs to be improved in the details of mask generation. The performance of the model in defect point detection is further

TABLE 1 Index values of different assessment methods.

Assessment method	IOU	AREA	MaxDets	Value 1	Value 2
AP	0.50–0.95	All	100	0.921	0.881
AP ₅₀	>0.50	All	100	0.934	0.926
AP ₇₅	>0.75	All	100	0.854	0.873
AP _s	0.50–0.95	Small	100	0.845	0.694
AP _m	0.50–0.95	Medium	100	0.896	0.811
AP _l	0.50–0.95	Large	100	0.912	0.976
AR _{m1}	0.50–0.95	All	1	0.632	0.694
AR _{m10}	0.50–0.95	All	10	0.726	0.789
AR _{m100}	0.50–0.95	All	100	0.791	0.804
AR _s	0.50–0.95	Small	100	0.751	0.792
AR _m	0.50–0.95	Medium	100	0.887	0.834
AR _l	0.50–0.95	Large	100	0.898	0.942

analyzed, and the overall Q&M requirements of the substation are met, and the detection effect is good. In the detection of objects with a pixel area greater than 96^2 , AP and AR are 97.6% and 94.2%, respectively. The model performs best. It can be seen that the model has a high detection accuracy rate for large insulator defect points, and has a good recall rate.

5 Conclusion

This work takes the intelligent Q&M of the equipment in the substation as the background and comprehensively analyzes the characteristics of the massive images of inspection insulators and the complex background of defect point detection. An intelligent detection method for substation insulator defects based on CenterMask is proposed. The proposal of this technology improves the efficiency and accuracy of insulator defect detection to a certain extent. The results of the example analysis verify the following main conclusion:

- 1) An end-to-end insulator defect point detection architecture is designed. The entire learning process does not perform artificial sub-problem division, but the deep learning model directly learns the mapping from the original input to the desired output.
- 2) It is only necessary to input the insulator field image captured by the inspection robot into the defect detection model. The three key tasks of target feature extraction, mask segmentation, and defect point target detection of insulators can be realized at one time.
- 3) A new agile detection method for insulator defects in substations is proposed. In the manual inspection mode, the waste of human resources and the potential safety hazards caused by the operation of the power grid are effectively reduced.

The transfer application research of this method will be the next exploration direction. It will greatly promote the efficiency and intelligence of substation equipment Q&M and has important research significance and engineering application value. At the same time, although the defect detection accuracy of this method is satisfactory, the hyperparameters involved in the optimal state of the model are still determined manually. Determining hyperparameters through model self-learning is a meaningful work.

Data availability statement

The original contributions presented in the study are included in the article/Supplementary Material; further inquiries can be directed to the corresponding author.

Author contributions

BY: designed this study. FL: contributed to the architecture of the insulator defect intelligent detection method. ML: contributed to the insulator feature extraction based on improved VoVNet. PY: contributed to the insulator mask extraction based on SAG-mask. HY: performed the identification and location of insulator defects based on FCOS. LW: collected and cleansed the data. All authors contributed to the writing of the article and all agreed to the submitted version of the article.

Conflict of interest

The authors declare that the research was conducted in the absence of any commercial or financial relationships that could be construed as a potential conflict of interest.

Publisher's note

All claims expressed in this article are solely those of the authors and do not necessarily represent those of their affiliated

organizations, or those of the publisher, the editors, and the reviewers. Any product that may be evaluated in this article, or claim that may be made by its manufacturer, is not guaranteed or endorsed by the publisher.

References

- Chen, J., Xu, X., and Dang, H. (2019). Fault detection of insulators using second-order fully convolutional network model. *Math. Problems Eng.* 2019, 1–10. doi:10.1155/2019/6397905
- Du, Y., Du, L., and Li, L. (2021). An SAR target detector based on gradient harmonized mechanism and attention mechanism. *IEEE Geosci. Remote Sens. Lett.* 19, 1–5. doi:10.1109/LGRS.2021.3103378
- Gao, Z., Yang, G., Li, E., and Liang, Z. (2021). Novel feature fusion module-based detector for small insulator defect detection. *IEEE Sens. J.* 21 (15), 16807–16814. doi:10.1109/JSEN.2021.3073422
- Guan, X., Gao, W., Peng, H., Shu, N., and Gao, D. W. (2021). Image-based incipient fault classification of electrical substation equipment by transfer learning of deep convolutional neural network. *IEEE Can. J. Electr. Comput. Eng.* 45 (1), 1–8. doi:10.1109/ICJECE.2021.3109293
- Han, S., Yang, F., Jiang, H., Yang, G., Zhang, N., and Wang, D. (2021). A smart thermography camera and application in the diagnosis of electrical equipment. *IEEE Trans. Instrum. Meas.* 70, 1–8. doi:10.1109/TIM.2021.3094235
- He, J., and Gorur, R. S. (2017). Flashover of insulators in a wet environment. *IEEE Trans. Dielectr. Electr. Insul.* 24 (2), 1038–1044. doi:10.1109/TDEL.2017.005795
- Huang, Q., Jing, S., Li, J., Cai, D., Wu, J., and Zhen, W. (2016). Smart substation: State of the art and future development. *IEEE Trans. Power Deliv.* 32 (2), 1098–1105. doi:10.1109/TPWRD.2016.2598572
- Jin, L., Tian, Z., Ai, J., Zhang, Y., and Gao, K. (2018). Condition evaluation of the contaminated insulators by visible light images assisted with infrared information. *IEEE Trans. Instrum. Meas.* 67 (6), 1349–1358. doi:10.1109/TIM.2018.2794938
- Kou, L., Li, Y., Zhang, F., Gong, X., Hu, Y., Yuan, Q., et al. (2022). Review on monitoring, operation and maintenance of smart offshore wind farms. *Sensors* 22 (8), 2822. doi:10.3390/s22082822
- Kou, L., Liu, C., Cai, G. W., Zhang, Z., Zhou, J. N., and Wang, X. M. (2020b). Fault diagnosis for three-phase PWM rectifier based on deep feedforward network with transient synthetic features. *ISA Trans.* 101, 399–407. doi:10.1016/j.isatra.2020.01.023
- Kou, L., Liu, C., Cai, G. W., Zhou, J. N., Yuan, Q. D., and Pang, S. M. (2020a). Fault diagnosis for open-circuit faults in NPC inverter based on knowledge-driven and data-driven approaches. *IET Power Electron.* 13 (6), 1236–1245. doi:10.1049/iet-pel.2019.0835
- Lee, Y., and Park, J. (2020). “Centermask: Real-time anchor-free instance segmentation,” in *Proceedings of the IEEE/CVF conference on computer vision and pattern recognition*, 13906–13915. doi:10.1109/CVPR42600.2020.01392
- Li, Y., Li, J., and Wang, Y. (2022d). Privacy-preserving spatiotemporal scenario generation of renewable energies: A federated deep generative learning approach. *IEEE Trans. Ind. Inf.* 18 (4), 2310–2320. doi:10.1109/TII.2021.3098259
- Li, Y., Li, K., Yang, Z., Yu, Y., Xu, R., and Yang, M. (2022b). Stochastic optimal scheduling of demand response-enabled microgrids with renewable generations: An analytical-heuristic approach. *J. Clean. Prod.* 330, 129840. doi:10.1016/j.jclepro.2021.129840
- Li, Y., Li, Z., and Chen, L. (2019). Dynamic state estimation of generators under cyber attacks. *IEEE Access* 7, 125253–125267. doi:10.1109/ACCESS.2019.2939055
- Li, Y., Wang, B., Yang, Z., Li, J., and Chen, C. (2022c). Hierarchical stochastic scheduling of multi-community integrated energy systems in uncertain environments via Stackelberg game. *Appl. Energy* 308, 118392. doi:10.1016/j.apenergy.2021.118392
- Li, Y., Zhang, M., and Chen, C. (2022a). A deep-learning intelligent system incorporating data augmentation for short-term voltage stability assessment of power systems. *Appl. Energy* 308, 118347. doi:10.1016/j.apenergy.2021.118347
- Shi, Z. B., Li, Y., and Yu, T. (2009). “Short-term load forecasting based on LS-SVM optimized by bacterial colony chemotaxis algorithm,” in 2009 International Conference on Information and Multimedia Technology, 306–309. doi:10.1109/ICIMT.2009.57
- Shi, Z. B., Yu, T., Zhao, Q., Li, Y., and Lan, Y. B. (2008). Comparison of algorithms for an electronic nose in identifying liquors. *J. Bionic Eng.* 5 (3), 253–257. doi:10.1016/S1672-6529(08)60032-3
- Tang, S., Zhou, P., Wang, X., Yu, Y., and Li, H. (2020). Design and experiment of dry-ice cleaning mechanical arm for insulators in substation. *Appl. Sci.* 10 (7), 2461. doi:10.3390/app10072461
- Tao, X., Zhang, D., Wang, Z., Liu, X., Zhang, H., and Xu, D. (2018). Detection of power line insulator defects using aerial images analyzed with convolutional neural networks. *IEEE Trans. Syst. Man, Cybern. Syst.* 50 (4), 1486–1498. doi:10.1109/TSMC.2018.2871750
- Usamentiaga, R., Fernandez, M. A., Villan, A. F., and Carus, J. L. (2018). Temperature monitoring for electrical substations using infrared thermography: Architecture for industrial internet of things. *IEEE Trans. Ind. Inf.* 14 (12), 5667–5677. doi:10.1109/TII.2018.2868452
- Wang, B., Dong, M., Ren, M., Wu, Z., Guo, C., Zhuang, T., et al. (2020a). Automatic fault diagnosis of infrared insulator images based on image instance segmentation and temperature analysis. *IEEE Trans. Instrum. Meas.* 69 (8), 5345–5355. doi:10.1109/TIM.2020.2965635
- Wang, H., and Meng, F. (2019). Research on power equipment recognition method based on image processing. *EURASIP J. Image Video Process.* 2019 (1), 57–11. doi:10.1186/s13640-019-0452-5
- Wang, H., Zhou, B., and Zhang, X. (2017). Research on the remote maintenance system architecture for the rapid development of smart substation in China. *IEEE Trans. Power Deliv.* 33 (4), 1845–1852. doi:10.1109/TPWRD.2017.2757939
- Wang, S., Liu, Y., Qing, Y., Wang, C., Lan, T., and Yao, R. (2020b). Detection of insulator defects with improved resnest and region proposal network. *IEEE Access* 8, 184841–184850. doi:10.1109/ACCESS.2020.3029857
- Xu, D., and Wu, Y. (2020). Improved YOLO-V3 with DenseNet for multi-scale remote sensing target detection. *Sensors* 20 (15), 4276. doi:10.3390/s20154276
- Yuan, Q., Zhang, Z., Pi, Y., Kou, L., and Zhang, F. (2021). Real-time closed-loop detection method of vSLAM based on a dynamic siamese network. *Sensors* 21 (22), 7612. doi:10.3390/s21227612
- Zhai, Y., Chen, R., Yang, Q., Li, X., and Zhao, Z. (2018). Insulator fault detection based on spatial morphological features of aerial images. *IEEE Access* 6, 35316–35326. doi:10.1109/ACCESS.2018.2846293
- Zhang, D., and Chen, S. (2020). Intelligent recognition of insulator contamination grade based on the deep learning of ultraviolet discharge image information. *Energies* 13 (19), 5221. doi:10.3390/en13195221
- Zhang, K., Qian, S., Zhou, J., Xie, C., Du, J., and Yin, T. (2022). ARFNet: Adaptive receptive field network for detecting insulator self-explosion defects. *Signal Image Video process.*, 1–9. doi:10.1007/s11760-022-02186-3
- Zhao, Z., Zhen, Z., Zhang, L., Qi, Y., Kong, Y., and Zhang, K. (2019). Insulator detection method in inspection image based on improved faster R-CNN. *Energies* 12 (7), 1204. doi:10.3390/en12071204